

## Structure and dynamics of surface crystallization of liquid $n$ -alkanes

T. K. Xia and Uzi Landman

*School of Physics, Georgia Institute of Technology, Atlanta, Georgia 30332*

(Received 22 March 1993)

Formation of a crystalline monolayer at the surface of an adsorbed liquid  $n$ -heptadecane film above the bulk solidification temperature, with the molecules in the layer hexagonally packed and their axes tilted by  $\sim 25^\circ$  from the surface normal, is found using molecular-dynamics simulations, corroborating recent observations. A crystallized adsorbed thin film ( $\sim 40$  Å) of hexadecane is found to consist of four layers of molecules oriented parallel to the substrate and a topmost hexagonally packed layer with molecules oriented toward the normal.

### I. INTRODUCTION

The structure and rich phase behavior in the bulk of linear hydrocarbon chain systems, known as  $n$ -alkanes ( $C_nH_{2n+2}$ ), have been quite thoroughly investigated.<sup>1</sup> However, while of significant fundamental as well as applied interest in diverse areas (such as statistical mechanics of complex fluids, thin-film boundary lubrication, and certain biological systems), explorations of the properties of interphase interfaces of these systems [solid-to-liquid (sl) and liquid-to-vapor (lv)] are less abundant. In this context we call attention to the fundamental distinction between ordering processes and other properties of  $n$ -alkane systems and those of the much studied Langmuir-Blodgett (LB) and self-assembled films,<sup>2</sup> where in the  $n$ -alkane case exchange between surface and bulk molecules can occur with relative ease while in the latter systems anchoring to the surface and insolubility of the amphiphile molecules induce ordering.

Recently, detailed atomic and molecular-scale information pertaining to structure, dynamics, and phases of interfacial alkane systems has been obtained with the use of tip microscopies<sup>3</sup> [scanning tunneling microscopy (STM) and atomic force microscopy (AFM)], the surface force apparatus (SFA),<sup>4</sup> surface tension measurements,<sup>5,6</sup> x-ray reflectivity (XR),<sup>4</sup> and grazing-incidence diffraction (GID),<sup>6</sup> and large-scale molecular-dynamics (MD) simulations.<sup>3(b),7-11</sup> These investigations revealed lamellar intermolecular structures of adsorbed alkane monolayers with the molecules lying predominantly in the surface plane.<sup>3,7,9</sup> They also revealed the layered nature of the density profile of interfacial and confined alkane films,<sup>3(b),4,10,11</sup> oscillatory force as a function of distance (film thickness) between the confining boundaries,<sup>3(b),4,10</sup> the energetics and structure of liquid junctions,<sup>10</sup> drainage and rheological properties and their dependence on the nature of surface-liquid interaction and on load and shear rates,<sup>4,11</sup> structural characteristics of the density and molecular arrangements at sl and lv interfaces,<sup>3,7,10,11</sup> enhanced diffusion at the lv interface,<sup>7</sup> and, most recently, surface-induced phase transitions investigated via XR, GID,<sup>6</sup> and surface-tension measurements.<sup>5,6</sup> In the latter measurements,<sup>6</sup> formation of a hexagonally packed crystalline monolayers at the surface of  $n$ -alkane liquids above the bulk solidification tempera-

ture, with the alkane molecules oriented normal to the surface,<sup>6</sup> is exhibited.

We report on extensive MD simulations of adsorbed liquid  $n$ -alkane films ( $n = 16$  and  $17$ ) that predict and provide characterization of the microscopic structure and dynamics of surface-induced crystallization in these systems, and corroborate recent observations.<sup>6</sup> In Sec. II we provide pertinent details of our simulations and in Sec. III we present our results.

### II. METHOD

In our simulations we investigated  $n$ -C<sub>16</sub>H<sub>34</sub> and  $n$ -C<sub>17</sub>H<sub>36</sub> films (thickness  $d_{th} \sim 40$  and  $90$  Å, respectively) adsorbed on a crystalline substrate [modeling Au(001)], at various temperatures. The areas of the calculational cells, which were periodically repeated in the  $x$ - $y$  directions parallel to the surface [with no periodicity applied along the film thickness direction ( $z$ )], were  $3.745 \times 10^3$  Å<sup>2</sup> (i.e., a linear dimension of  $61.2$  Å); the total number of molecules in the calculational cell were  $N(C_{16}H_{34}) = 300$ , and  $N(C_{17}H_{36}) = 565$ .

The alkane systems were described via intramolecular and intermolecular interaction developed previously<sup>7,9,11</sup> [including intersegment (CH<sub>2</sub> and CH<sub>2</sub> pseudoatoms) interactions, dihedral, and bond-bending potentials]. The interactions with the substrate were modeled via 6-12 Lennard-Jones potentials, with parameters determined by fitting to experimentally estimated adsorption energies.<sup>7,11</sup> All other calculational details and the method of initial preparation and prolonged equilibration can be found elsewhere.<sup>7,11</sup>

In each simulation, we started from an equilibrated liquid film at high temperature ( $T = 350$  K for  $n$ -C<sub>16</sub>H<sub>34</sub> and  $T = 373$  K for  $n$ -C<sub>17</sub>H<sub>36</sub>; the corresponding experimental melting temperatures are  $T_m = 291.32$  and  $295.15$  K, respectively), and cooled the system to the desired temperature via stochastic thermalization of the particles' velocities. Equilibrium simulations lasted 1600 ps, and averaging of data was performed over the last 200 ps. We note that our simulation times are very long by current MD standards for such complex systems. Inspection of various characteristics of the systems (energetics, structure, and transport) leads us to conclude that equilibrium has been achieved at each of the temperatures we report.

### III. RESULTS

Calculated density profiles, order parameters, and diffusion constants for  $n$ -C<sub>16</sub>H<sub>34</sub> and  $n$ -C<sub>17</sub>H<sub>36</sub> at high and low temperatures are shown in Fig. 1. As discussed by us previously,<sup>7</sup> the high-temperature lv interfacial profiles can be fit by an error function and the average segmental distribution of the  $z$ -height fluctuations can be fit by a Gaussian with a width  $\sim 3$  Å, implying a short correlation length in the surface region.

The calculated surface tensions  $\sigma$ [C<sub>16</sub>H<sub>34</sub>]=22.3 dyn/cm and  $\sigma$ [C<sub>17</sub>H<sub>36</sub>]=22.3 dyn/cm, at  $T=350$  and 373 K, respectively, are in good agreement with experimental values<sup>12</sup> ( $22.58 \pm 0.1$  and 21.14 dyn/cm, respectively). At the lower temperature,  $T$ (C<sub>16</sub>H<sub>34</sub>)=288.3 K and  $T$ (C<sub>17</sub>H<sub>36</sub>)=297.15 K, the whole hexadecane film is crystallized [below  $T_m$ (C<sub>16</sub>H<sub>34</sub>)], while the density profile for the heptadecane film exhibits an increased density region at the lv interface, and a bulklike region as well as layered density oscillations at the sl interface [the development of the density enhancement at the lv interface starts at  $T_m + (4 \pm 1)$  K for both the alkane systems; in addition the calculated surface tension for the heptade-

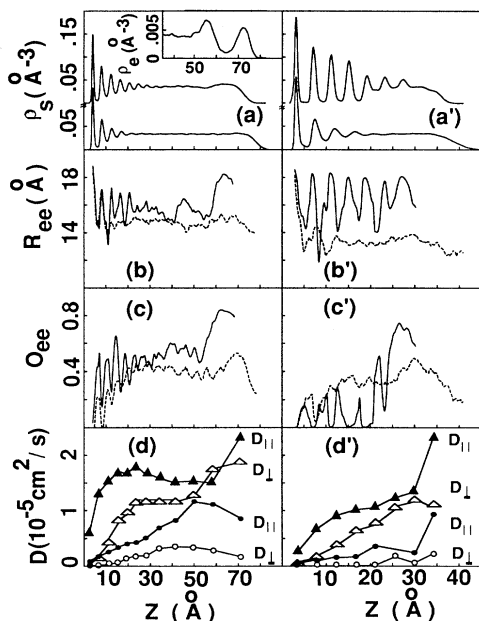


FIG. 1. Profiles vs distance away from the solid Au(001) surface ( $z$ ) of segmental density ( $\rho_s$ ) at two temperatures: 373 K (bottom) and 297.15 K (top) for  $n$ -C<sub>17</sub>H<sub>36</sub> in (a), and 350 K (bottom) and 288.3 K (top) for  $n$ -C<sub>16</sub>H<sub>34</sub> in (a'), the latter corresponding to an almost fully crystallized film. A profile of the density of molecule end segments ( $\rho_e$ ) is shown in the inset of (a). Distributions of end-to-end lengths [ $R_{ee}(z)$ , in (b) and (b')] and orientational order parameters [ $O_{ee}(z)$ , in (c) and (c')], for  $n$ -C<sub>17</sub>H<sub>36</sub> and  $n$ -C<sub>16</sub>H<sub>34</sub> at the corresponding high (dashed line) and low (solid line) temperatures. Diffusion coefficients (parallel  $D_{||}$ , and normal  $D_{\perp}$  to the surface) are shown in (d) and (d'). Empty and filled triangles correspond to high-temperature films and empty and filled circles to low-temperature films, for  $n$ -C<sub>17</sub>H<sub>36</sub> and C<sub>16</sub>H<sub>34</sub> in (d) and (d'), respectively.

cane system exhibits an increase upon cooling; 22.3, 26.3, and 28.4 dyn/cm for  $T=373$ , 310, and 300 K, respectively, increasing further for  $T=297.15$  K and then decreasing at 295.15 K, in agreement with experimentally observed trends for this and other  $n$ -alkanes<sup>5,6</sup>]. While we have not determined the precise bulk melting for our systems, our extensive simulations have shown that above 295 and 300 K for hexadecane and heptadecane, respectively, both systems are in a liquid state. Consequently, it is safe to assume that the theoretical melting points for these systems are close to those determined experimentally. Moreover, as discussed above, the simulated hexadecane system solidified at 288.3 K (that is, below the experimental melting point).

The nature of ordering and dynamics in our systems is

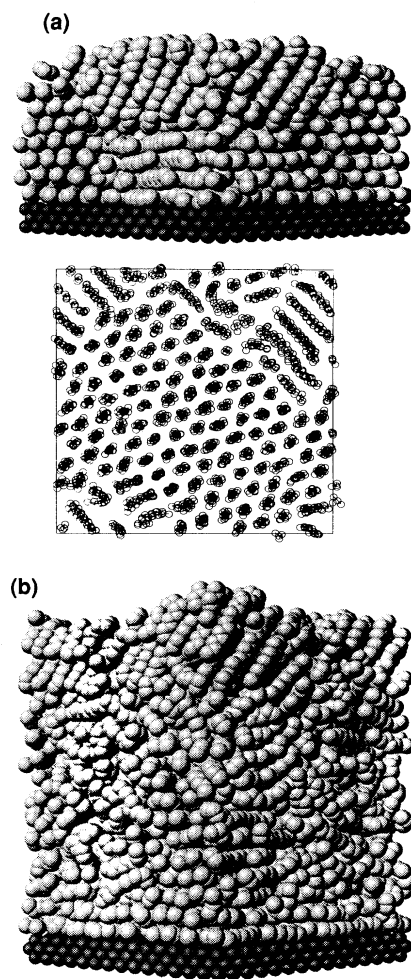


FIG. 2. Side view of the crystallized  $n$ -hexadecane film [in (a)] at 288.3 K, and a short-time trajectory of the surface viewed from above, illustrating hexagonal packing in an almost completely crystallized layer. (b) Side view of  $n$ -heptadecane recorded during the crystallization of a monolayer at the lv interface, on top of a liquid, at 297.15 K. The dimensions of the calculational cells in the directions parallel to the surface are 61.2 Å.

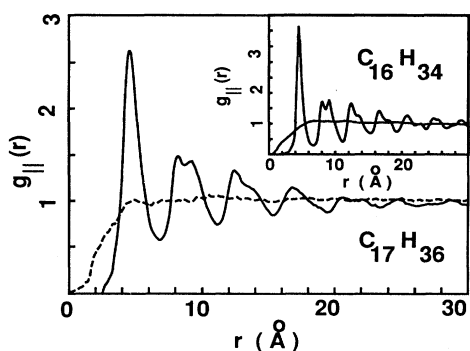


FIG. 3. Two-dimensional segmental pair-distribution functions of molecules in the topmost regions of  $n$ - $C_{17}H_{36}$  and  $n$ - $C_{16}H_{34}$  (inset), recorded at the corresponding high (dashed line) and low (solid line) temperatures of the films. For both films the ratios of the locations of maxima at the lower temperature  $g_{\parallel}(r)$  correspond to hexagonal close packing in the top layer. Distance is in  $\text{\AA}$ .

revealed by the order-parameter profiles,  $O_{ee}(z) = |\langle \mathbf{R}_{ee}(z) \cdot \hat{z} / R_{ee} \rangle|^2$  measuring the orientation of the molecular end-to-end vectors with respect to the surface normal ( $\hat{z}$ ), with  $R_{ee}(z)$  representing the end-to-end length distribution, and the diffusion coefficients parallel ( $D_{\parallel}$ ) and normal ( $D_{\perp}$ ) to the surface. In the above definitions,  $\mathbf{R}_{ee}$  is the vector connecting the two end segments of a molecule, and the angular brackets denote an average over all molecules whose center of mass are found in an averaging interval centered at  $z$ .

Both  $R_{ee}(z)$  and  $O_{ee}(z)$  show that for the crystallized  $n$ - $C_{16}H_{34}$  film (at  $T = 288.3$  K), molecules in the first four layers lie preferentially parallel to the surface [see  $z < 20$   $\text{\AA}$  in Fig. 1(c')], in a stretched conformation ( $R_{ee} \sim 18$   $\text{\AA}$ ; [Fig. 1(b')], which is close to the end-to-end length of the stretched molecule), while in the topmost crystalline layer the molecules are oriented normal to the surface in a stretched conformation [see also Fig. 2(a)]. Furthermore, from the two-dimensional pair-distribution function  $g_{\parallel}(r)$  shown in Fig. 3 (inset) (and analysis of the  $O_6$  order-parameter profile,<sup>13</sup> measuring segmental 2D orientational order, not shown) we conclude that the molecules in the topmost crystalline layer are hexagonally packed (see also Fig. 2).

For the  $n$ - $C_{17}H_{36}$  film we observe that at  $T = 297.15$  K (that is, above the experimental bulk melting point) the topmost layer is characterized by a high degree of crystalline order with the stretched molecules tilted toward the normal (at an angle of  $25^\circ$ ) and their molecular axis parallel to each other (see inset of Fig. 1(a), displaying a profile of the molecular end-segment distribution [ $\rho_e(z)$ ], and Figs. 1(b), 1(c), and 2(b)). As in the case of the hexadecane film,  $g_{\parallel}(r)$  (see Fig. 3), as well as the  $O_6$  order parameter (not shown), indicate hexagonal packing in this surface crystallized layer.

The region below the surface crystallized monolayer of the  $n$ - $C_{17}H_{36}$  film exhibits liquid-state characteristics (the order parameters in this region are similar to those of the

hot liquid shown in Fig. 1; see also Fig. 2). Additionally, the layered nature of the sl interface, with the molecules oriented preferentially parallel to the surface, exhibiting extended regions of intermolecular order, are evident.

Along with the above structural characteristics, we note the spatial variation of the diffusion coefficients in the films, and their dependence on temperature. In the high-temperature liquid state, both films exhibit enhanced diffusion as a function of increasing distance from the sl interface [Figs. 1(d) and 1(d')]. At low temperatures diffusion is decreased, and for the  $n$ -heptadecane film we observe liquidlike diffusion characteristics in the middle, bulklike, region, with reduced values in the sl interface and the surface crystallized monolayer [Fig. 1(d)]; in the crystallized hexadecane film diffusion is small throughout, with a slight enhancement of  $D_{\parallel}$  near the solid-to-vapor interface [see Fig. 1(d')].

#### IV. SUMMARY

The structural and dynamical properties predicted and revealed by our simulations corroborate and support the interpretation of recent experimental observations where a first-order surface-induced crystallization transition of a monolayer of molecules oriented preferentially toward the surface normal and packed in a hexagonal lattice, occurring above the bulk solidification temperature, was suggested.<sup>6</sup> In this context, we note early observations on liquid-metal surfaces,<sup>14</sup> which were interpreted as evidence of surface-induced crystallization of up to three topmost layers at the lv surface, as well as observations of ordering at sodium dodecylsulphate (SDS)/water solutions.<sup>15</sup>

Ordering and/or crystallization transitions are driven by lowering of the free energy, portraying contributions from energetic and entropic terms. For liquid-metal surfaces, considerations related to embedding of ions in the conduction-electron density have been invoked in order to explain a positive temperature coefficient  $\partial\sigma/\partial T$  corresponding to low-entropy states associated with ordering near the surface of liquid metals above the freezing point.<sup>14</sup>  $n$ -alkanes, which are among the simplest complex fluids, provide a testing ground of concepts and theories pertaining to the relative importance of energy and entropy contributions via systematic investigations of  $C_nH_{2n+2}$  systems with varying chain length, as well as studies of alkane mixtures and effects due to modifications of molecular topology (i.e., iso-alkanes, where deviations from linearity are introduced by side chains). Explorations along these lines are in progress in our laboratory.

#### ACKNOWLEDGMENT

Research was supported by the U.S. Department of Energy, the Air Force Office of Scientific Research, and the National Science Foundation. We gratefully acknowledge allocation of computer time on the Cray C-90 at the Pittsburgh Supercomputing Center, where most of the simulations were performed.

- <sup>1</sup>D. M. Small, *The Physical Chemistry of Lipids* (Plenum, New York, 1986).
- <sup>2</sup>A. Ulman, *Ultrathin Organic Films* (Academic, San Diego, 1991).
- <sup>3</sup>(a) L. Askadskaya and J. P. Rabe, *Phys. Rev. Lett.* **69**, 1395 (1992); (b) U. Landman, W. D. Luedtke, J. Ouyang, and T. K. Xia, *Jpn. J. Appl. Phys.* **32**, 28 (1993); U. Landman and W. D. Luedtke, in *Scanning Tunneling Microscopy III*, edited by H. J. Guntherodt and R. Wiesebanger (Springer, Berlin, 1993), Chap. 9.
- <sup>4</sup>J. H. Israelachvili, *Intermolecular and Surface Forces*, 2nd ed. (Academic, London, 1992); H. K. Christenson *et al.*, *J. Chem. Phys.* **87**, 1834 (1987); S. Granick, *Science* **253**, 1374 (1991).
- <sup>5</sup>J. C. Earnshaw and C. J. Hughes, *Phys. Rev. A* **46**, 4494 (1992).
- <sup>6</sup>X. Z. Wu, E. B. Sirota, S. K. Sinha, B. M. Ocko, and M. Deutsch, *Phys. Rev. Lett.* **70**, 958 (1993).
- <sup>7</sup>T. K. Xia, J. Ouyang, M. W. Ribarsky, and U. Landman, *Phys. Rev. Lett.* **69**, 1967 (1992).
- <sup>8</sup>J. Harris, *J. Phys. Chem.* **96**, 5077 (1992).
- <sup>9</sup>S. Leggetter and D. J. Tildesley, *Mol. Phys.* **68**, 519 (1989).
- <sup>10</sup>W. D. Luedtke and U. Landman, *Comput. Mater. Sci.* **1**, 1 (1992).
- <sup>11</sup>M. W. Ribarsky and U. Landman, *J. Chem. Phys.* **97**, 1937 (1992), and references therein.
- <sup>12</sup>J. J. Jasper, *J. Phys. Chem. Ref. Data* **1**, 841 (1972).
- <sup>13</sup>D. R. Nelson and B. I. Halperin, *Phys. Rev. B* **19**, 2457 (1979); C. L. Cleveland, C. S. Brown, and U. Landman, *Phys. Rev. Lett.* **45**, 2032 (1980).
- <sup>14</sup>C. A. Croxton, *Statistical Mechanics of the Liquid Surface* (Wiley, New York, 1980); see also E. T. Chen, R. N. Barnett, and U. Landman, *Phys. Rev. B* **40**, 924 (1989), where an increased degree of order at the lv interface of nickel is discussed.
- <sup>15</sup>B. Berge, L. Fancheux, K. Schwab, and A. Libchaber, *Nature (London)* **350**, 322 (1991).

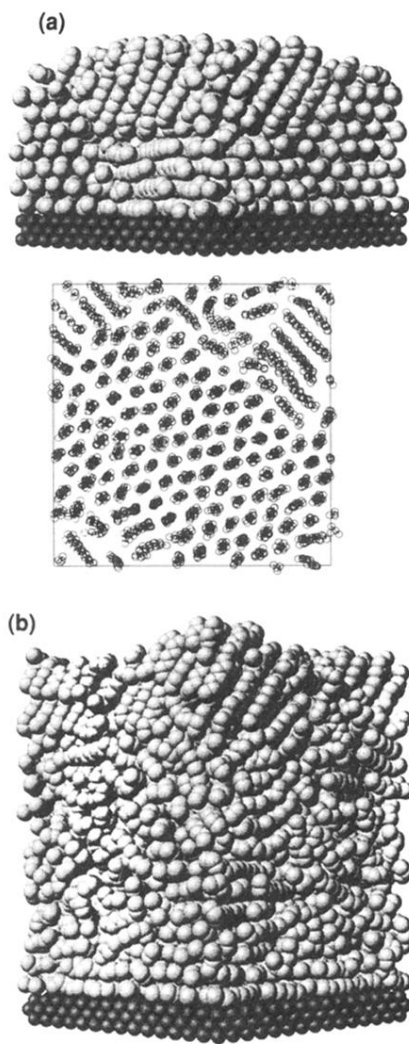


FIG. 2. Side view of the crystallized *n*-hexadecane film [in (a)] at 288.3 K, and a short-time trajectory of the surface viewed from above, illustrating hexagonal packing in an almost completely crystallized layer. (b) Side view of *n*-heptadecane recorded during the crystallization of a monolayer at the lv interface, on top of a liquid, at 297.15 K. The dimensions of the calculational cells in the directions parallel to the surface are 61.2 Å.